Supporting Information

Fan et al. 10.1073/pnas.1316830110

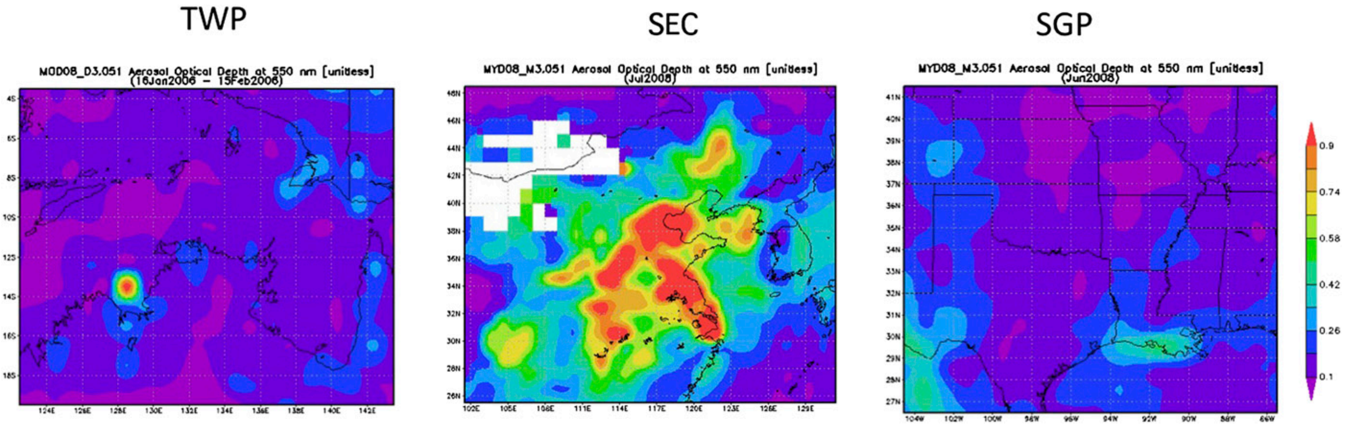

Fig. S1. Aerosol optical depth (AOD) averaged over the 1-mo time period at tropical western Pacific (TWP), southeastern China (SEC), and the U.S. southern Great Plains (SGP). At TWP and SGP, air is relatively clean with similar AODs in the range of 0.1–0.25, whereas AOD at SEC is more than 6 times larger in general.

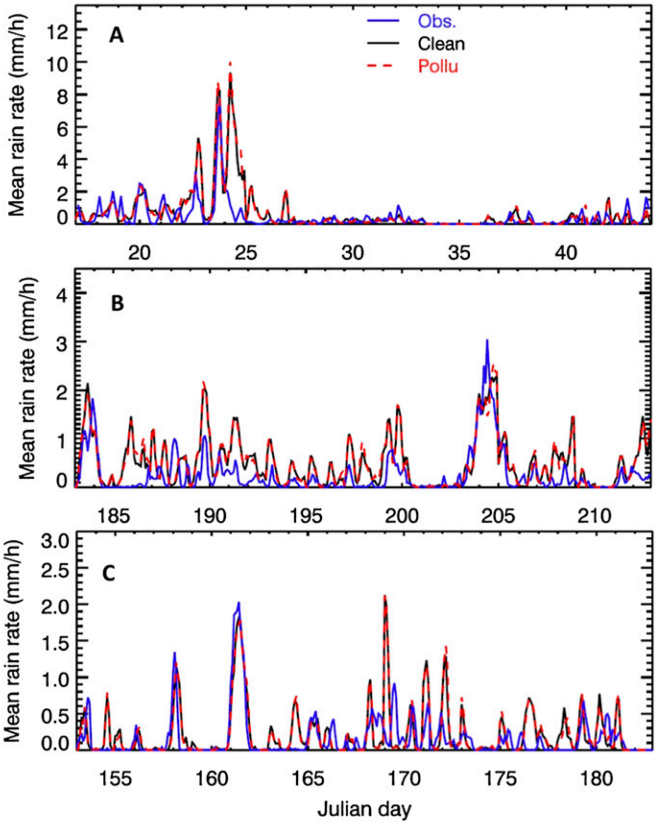

Fig. S2. Comparison of times series of rain rates from both clean and polluted simulations with observations at (*A*) TWP, (*B*) SEC, and (*C*) SGP. Refer to *Materials and Methods* for the data details.

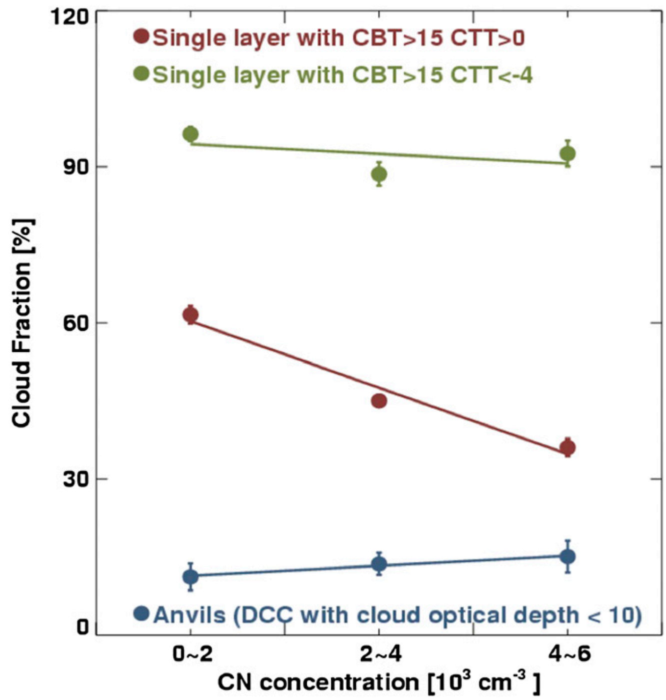

Fig. S3. Relationship between cloud fraction and surface aerosol number concentration at the SGP for shallow warm clouds (brown), deep convective cloud (DCC) core clouds (green), and anvil clouds associated with DCCs (blue). The results are obtained from 10 y of continuous measurements from 2000 through 2010. Cloud fractions are calculated as the ratio of the number of cloudy pixels over that of total pixels in the 20 km × 20 km field of view centered at the central facility site of SGP for an identified DCC. We further separate DCCs into a thick core part [pixels with cloud optical depth (τ) > 10] and an anvil part with τ < 10. CBT, cloud base temperature; CTT, cloud top temperature.

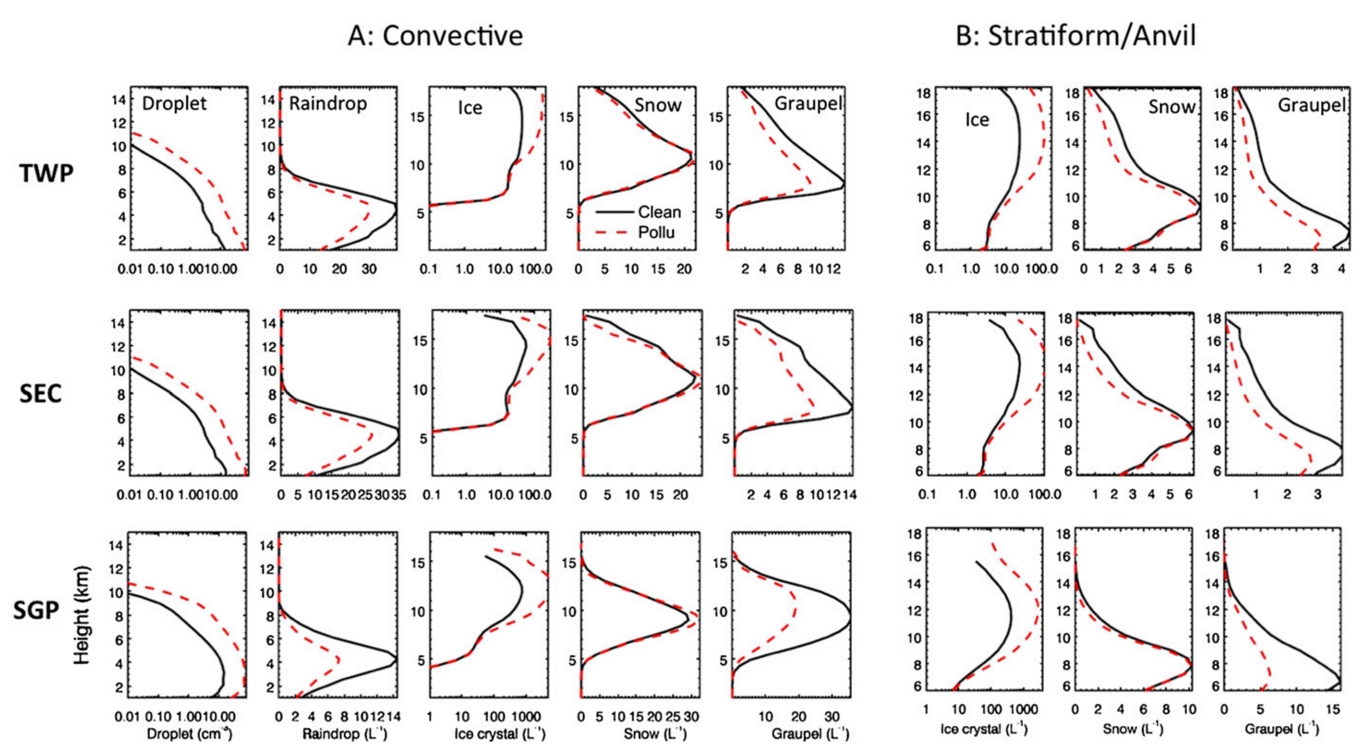

Fig. S4. Vertical profiles of number concentrations of hydrometeors for (*A*) the convective core area and (*B*) the stratiform/anvil regimes under clean (black) and polluted (red dashed) conditions. In the stratiform/anvil regimes, liquid water content is very small.

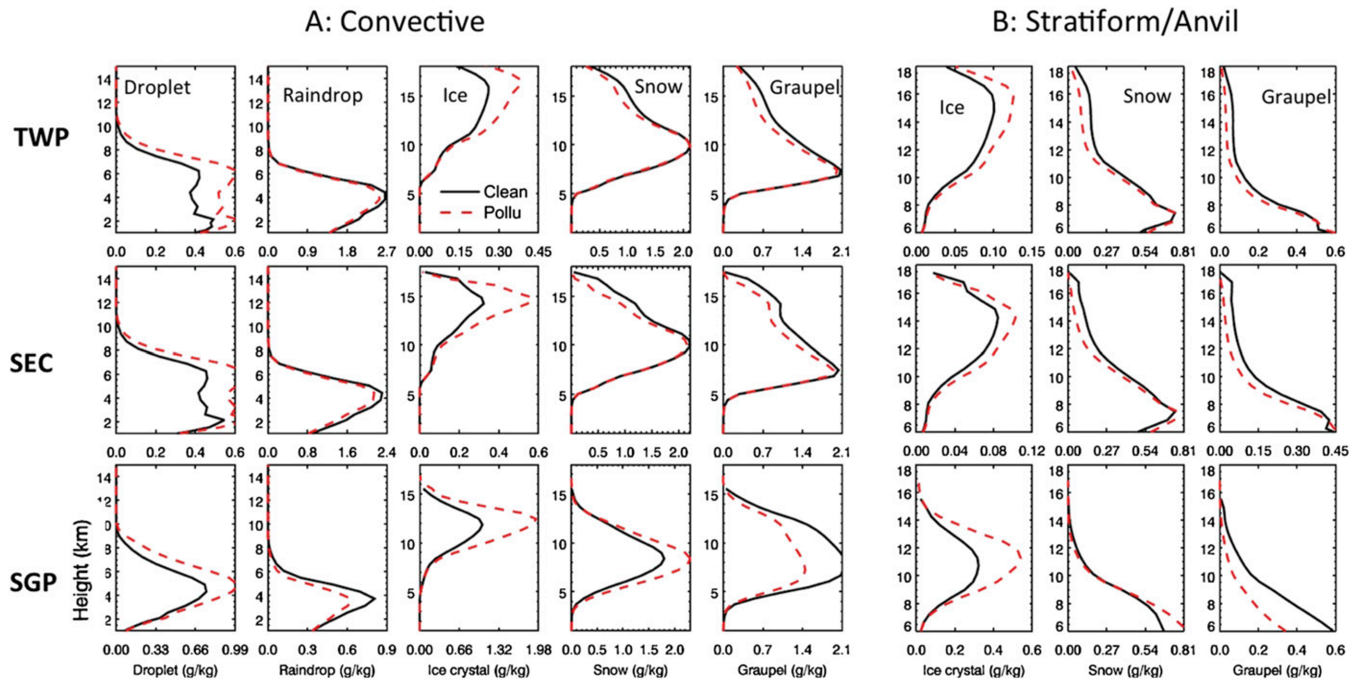

Fig. S5. Vertical profiles of mass concentrations of hydrometeors for (*A*) the convective core area and (*B*) the stratiform/anvil regimes under clean (black) and polluted (red dashed) conditions.

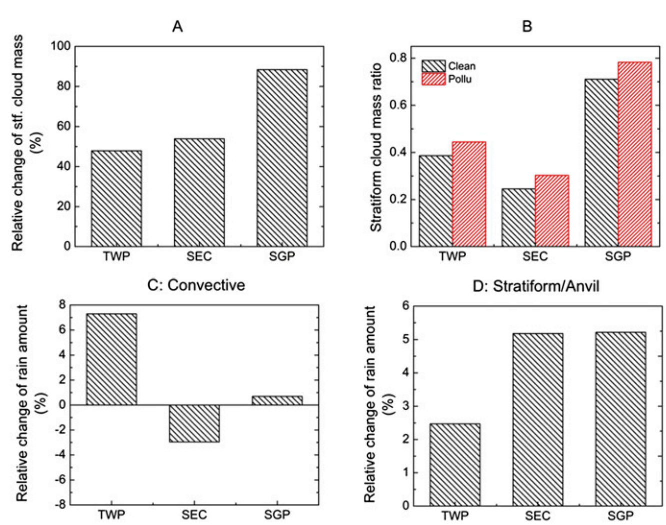

Fig. S6. Changes of (*A*) stratiform/anvil cloud mass (%) and (*B*) the cloud mass ratio in stratiform/anvil from the clean to the polluted conditions. Cloud mass is the sum of the mass concentrations of all hydrometeors (i.e., droplet, raindrop, ice, snow, and graupel) in the stratiform/anvil regimes. The stratiform cloud mass ratio is calculated as the cloud mass in the stratiform/anvil regimes divided by the total mass (i.e., the sum over core and stratiform/anvil). Relative changes of total rain amount (%) in 1 mo at (*C*) convective cores and (*D*) stratiform/anvil for TWP, SEC, and SGP (*x* axis). The changes at convective cores are not consistent, but the increase of stratiform rain is consistent among the three regions.

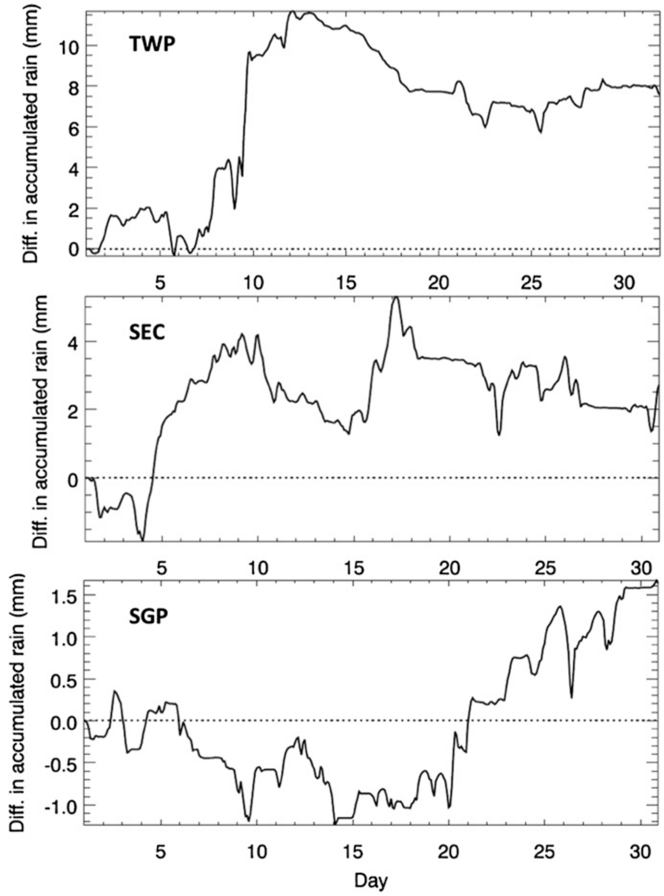

Fig. S7. Differences of the accumulated rain between polluted and clean conditions for (*Top*) TWP, (*Middle*) SEC, and (*Bottom*) SGP. The averaged rain per day ($mm \cdot d^{-1}$) in the clean and polluted conditions is 61.1 and 66.7 in TWP, 70.3 and 72.0 in SEC, 46.9 and 46.0 in SGP before day 21, and 33.9 and 37.4 in SGP after day 21, respectively, consistent with the changing trends of the accumulated rain from the clean to polluted conditions.

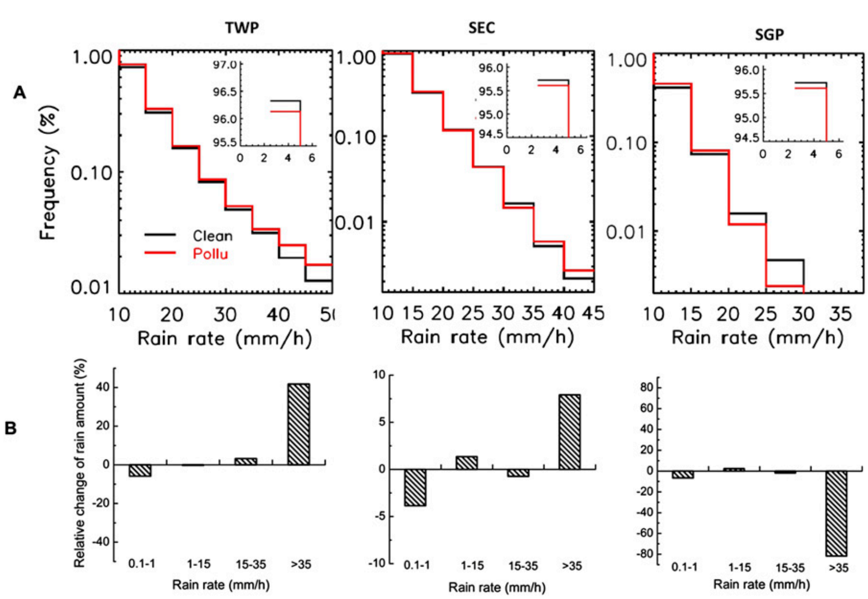

Fig. S8. Rain rate frequency and amount. (*A*) Probability distribution of rain rate frequency under clean (black) and polluted (red) conditions and (*B*) relative change in rain amount for TWP, SEC, and SGP.

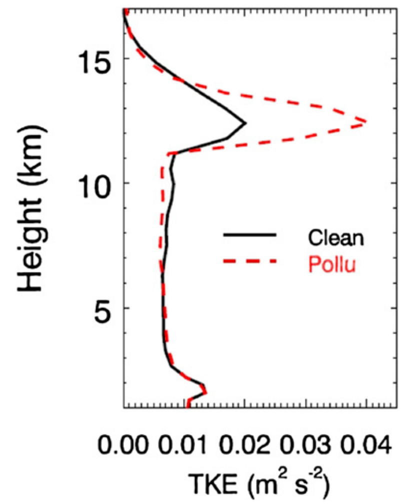

Fig. S9. Turbulence kinetic energy (TKE) from the clean (black) and polluted (red) environments at days 26–28 in TWP. Simulations for this period were rerun to output TKE.

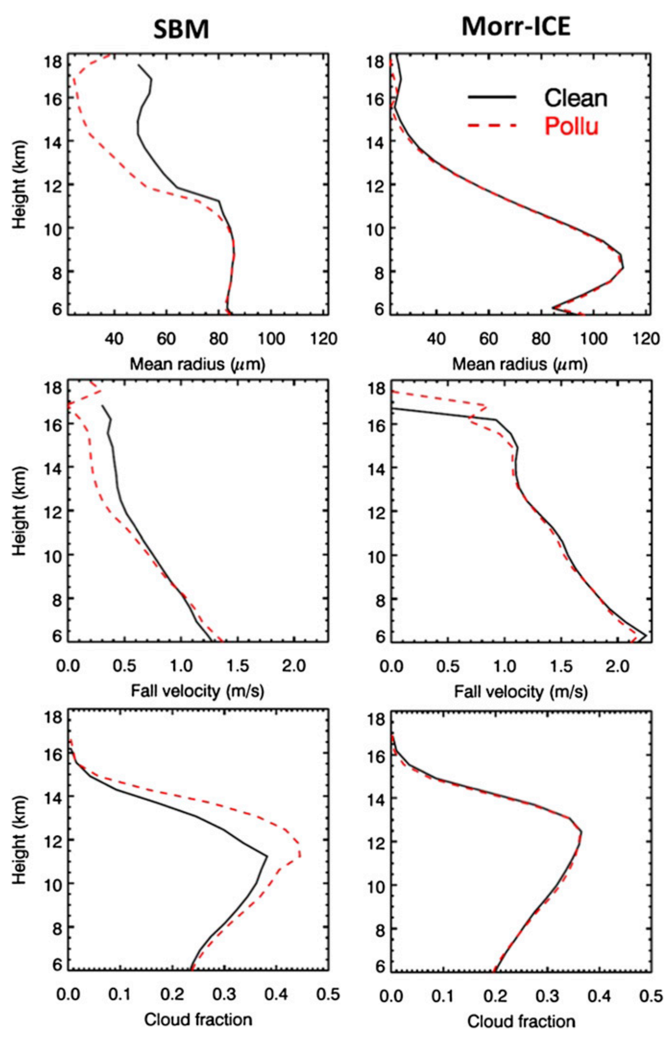

Fig. S10. Vertical profiles of mean radius of ice/snow (top row), fall velocity (middle row), and cloud fraction (bottom row) for simulations with spectral-bin microphysics (SBM) and a modified Morrison scheme (Morr-ice). Morr-ice has the same cloud condensation nuclei representations and ice nucleation parameterizations as SBM.